JALS Vol.2 n.1
Journal of Applied and Laser Spectroscopy 2015

Dynamics of Optical Breakdown in Tap and Pure Water Induced by λ=1064 nm 6 ns Laser Pulses

Grigory Toker, Valery Bulatov, Tatiana Kovalchuk and Israel Schechter

Schulich Faculty of Chemistry
Technion - Israel Institute of Technology, Haifa 32000, Israel
Israel@tx.technion.ac.il

Received 11/3/2015, accepted 08/05/2015

ABSTRACT

The processes accompanying optical breakdowns in tap and pure water and in their mixtures were visualized and measured by applying a high spatial resolution Mach-Zehnder interferometry technique. The breakdown events were directly related to inclusion particles. The fraction of particles undergoing breakdown was estimated and the values are different in the tested water samples. Comparison of the structure and dynamics of the laser plasma columns in the studied liquids was performed. The lengths of the plasma columns in a series of mixtures on pure and tap water was measured and compared to theoretic models. While the moving breakdown model reasonably fits the plasma column length in pure water, a modified expression was needed for tap water. Warmed channels in the water samples were observed in the focal volume of a focusing singlet and their temperatures and evolution times were established.

1. INTRODUCTION

Optical breakdown in water in the microsecond time regime was characterized a long time ago [1,2]. In these first studies and in some of the later performed experimental investigations, the structure and dynamics of the laser plasma columns in water could not be studied due to the low spatial resolution of the applied diagnostic techniques.
The structure of laser plasma columns in tap water and their dynamics at earlier (0-100 ns) time delays have been recently investigated by applying a high spatial resolution shadow and Schlieren optical diagnostic techniques [3-4]. It was found that at the earlier stage of breakdown the laser plasma column has essentially discrete character and consists of plasma balls, micro-bubbles and associated spherical micro shockwaves, surrounding the bubbles.
Distilled and de-ionized water are commonly believed to be a suitable model for an impurity-free dielectric medium in some biomedical applications, and are characterized by high breakdown thresholds (in the range of 100-1000 GW·cm^{-2}). In contrast, ordinary tap water, which has higher content of impurities, exhibits a lower threshold for breakdown for ns laser pulses.
In this paper, the processes accompanying optical breakdowns at λ=1064 nm in mixtures of pure and tap water were studied in the ns delay range. The required optical diagnosis was obtained by applying a high spatial resolution Mach-Zehnder interferometry. The purpose of these experiments was to compare the structure of the laser plasma columns in the tested liquids at over-threshold laser fluxes.

2. EXPERIMENTAL

The optical breakdown processes were visualized and measured using Mach-Zehnder interferometry. The scheme of the experiment is presented in Figure 1. The laser used for underwater generation of the laser plasma columns was a Nd:YAG laser (Quanta-Ray INDI-YAG, Spectra Physics, CA). Its basic harmonic pulses (λ = 1064 nm, duration 6 ns) were focused by a singlet of 75 mm focal length into a quartz cuvette filled with the water samples

Corresponding author: Israel Schechter, e-mail: Israel@tx.technion.ac.il
Keywords: Optical Breakdown, Laser, Shock Waves, Water

(refraction index of n = 1.33). The laser pulse energies were varied in the range of ε_{out} = 15 - 150 mJ. The diameter of the focal spot was evaluated as $2w_o$ ~ 70 μm. The laser flux of the energy absorbed in the focal spot achieved the value of about ~E_a = 10^3 J·cm^{-2}.

A second laser was used for probing the interaction events, at a controlled time delay: the second harmonic radiation (λ = 532 nm, 6 ns) of a Nd:YAG laser (Quanta-Ray INDI-YAG, Spectra Physics, CA) was applied for inspecting the region of study in a direction perpendicular to the light propagation of the first laser beam. Both laser systems were operated at single pulse mode and were synchronized using a pulse generator (BNC 555-8CG, Berkley Nucleonic Corp., Berkley, CA), with accuracy better than 6 ns. The synchronization was used for visualizing the dynamics of the plasma column at different controllable time delays between the heating and diagnostic laser pulses.

The Mach-Zehnder interferometer consisted of two beam splitting cubes and two flat mirrors as shown in Figure 1. The interferometric images were obtained using an optical collimation system, consisting of two objective lenses: ILOCA-Quinon, f = 50 mm and Jupiter-9, f = 85 mm. The interference was realized by sharp focusing the laser plasma in water on the sensitive area of a CMOS camera (Alpha-900, Sony). This full-frame (24x36.9 mm^2) sensor has 1890x1260 pixels, 12 μm each. The best resolution is ≈ 4.5 μm / pix. The time delays τ_d were measured between the fronts of the heating and diagnostic laser pulses.

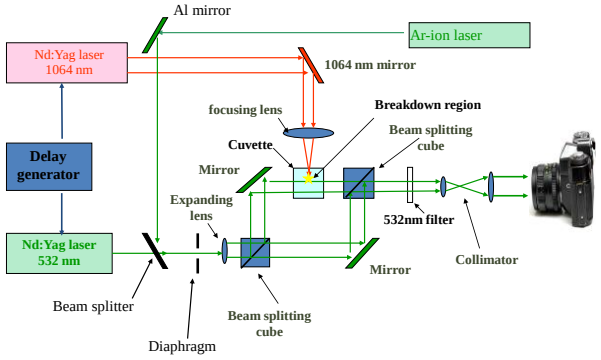

Figure 1: Experimental Mach Zehnder interferometry setup

The scattering radiation at 90 degrees provides information on the concentration of inclusions in the liquid. An argon-ion laser radiation (λ = 514.5 nm, ~1 mm diameter) tests the liquid in the 1x1x1 cm^3 cuvette. The scattered radiation in perpendicular direction was imaged on the CMOS sensor using a focusing system.

3. Results and Discussion

3.1 Structure and dynamics of laser plasma columns in water

The discrete structure of the laser plasma columns in tap and pure water is clearly observed in the interferograms presented in Figures 2 and 3. Two types of micro-objects are seen: (a) plasma micro-balls, (b) micro-bubbles, associated with spherical micro-shockwaves. Accurate analysis shows that the laser plasma columns consist of a train of the discussed objects, each of them presenting microscopic thermo-explosions of individual inclusions subjected to optical breakdown.

At the shortest time delays (of a few ns) the laser plasma column in *tap water* is filled with a train of small luminous micro-balls of about hundred μm diameter, as can be seen in Figure 2(a).

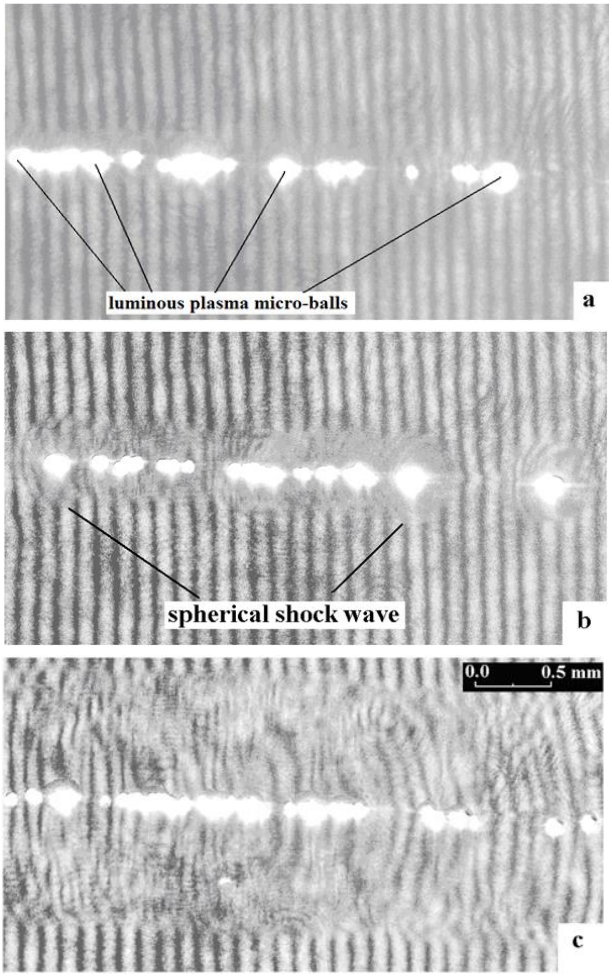

Figure 2: Fragments of interferograms of a laser plasma column in tap water at different time delays: (a) 7ns, (b) 52 ns, (c) 253ns.

A dozen nanoseconds later, micro-bubbles appear, as a result of the expansion of vapors surrounding the inclusion particles. The walls of the expanding bubbles generate the third objects in the laser plasma column: powerful spherical micro-shockwaves over the inclusion particles.

The structure of a laser spark column in *pure water* differs only numerically: the quantity of luminous micro-balls in the train is much smaller, due to the

small number of inclusions in the focal volume of the singlet. This speculation is confirmed in the series of interferograms presented in Figure 3. It is seen that the laser plasma columns may consist of two or even of a single micro-breakdown.

3.2 Mechanism of optical breakdown in tap and pure water

In 3.1 we showed that optical breakdown in water can be presented as a train of individual micro-breakdowns at discrete inclusion particles. Thus, the model of breakdown in water might be presented as a system of micro-explosions of individual inclusion particles located in the focal volume of the singlet.

Solid state particulates persistent in water are intensively illuminated by the focused laser beam. The surfaces of these inclusion particles begin to evaporate and at the same time the expanding motion of the vapors is strongly restricted by the surrounding water. This circumstance leads to high pressures in the inclusion vapors and creates favorable conditions for multiphoton transitions and cascade ionization [5]. The heating of the arising plasma is realized due to inverse bremsstrahlung process.

The discrete structure and dynamics of optical breakdown in tap water was previously investigated using high spatial resolution shadow and Schlieren diagnostic techniques [3]. However, high spatial resolution Mach-Zehnder interferometry allows us to verify the mechanism of the optical breakdown, by taking into account the explosive vaporization of the layer over the inclusions. The results are presented in the following.

The hot plasma creates a layer of evaporated material over the surface of the inclusion owing to the process of thermos-conductivity radiation. This spherical layer of vapors creates the bubble. The expanding walls of the bubble act as a spherical piston and effectively compress the surrounding water and thus generate the micro-spherical shockwave. The shockwave starts its expansion with supersonic velocity together with the bubble walls. After a few ns, the shockwave outdistances the walls of the bubble. Proper evaluation shows that the pressures in the shockwaves are in the Mbar range. Quickly after that, the micro-bubbles start to move with subsonic velocities. This range is presented in Figure 2(b). For longer delays the shockwaves also decay, moving with small supersonic velocities, transforming into strong acoustic waves, and finally move with the velocity of sound in water a_o = 1.46 km·s^{-1}. This time range is shown in Figure 2(c).

Both the bubbles and the associated shockwaves evolve in time, and their time dependent velocity and radius during the first 150 ns are shown in Figure 4. The Mach numbers presented in this Fig. were statistically averaged over all the train of particle's micro-explosions (up to two dozens of objects in tap water) for a given interferogram. The numbers were averaged again over ca. 10 interferograms obtained at the same time delay. It can be seen that maximal Mach number is approximately M = 4.7. This value corresponds to a pressure of 0.2 Mbar behind the front of the spherical shockwave.

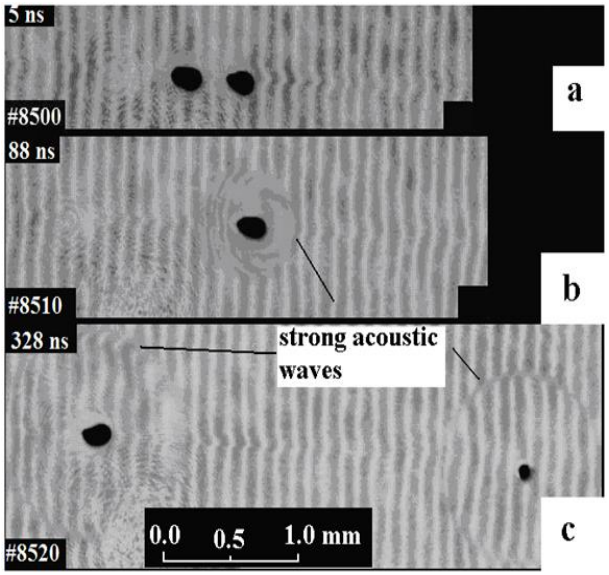

Figure 3: Dynamics of the optical breakdown in pure water (inverted images)

3.3 The fraction of inclusion particles undergoing breakdown

The fraction of particles in pure and tap water that undergo breakdown is also of interest. In order to calculate this fraction we have to estimate the concentration of breakdown events in the interaction volume and divide it by the total concentration of particles.

The lower boundary of the concentration of the breakdown inclusion particles might be evaluated in the following way. The interaction volume is a cylinder of diameter ≈ $2w_0$ and length of Rayleigh length, z_R.

$$z_R = \frac{2\pi n}{\lambda} w_0^{\,2} \approx 0.96 \text{ cm}$$

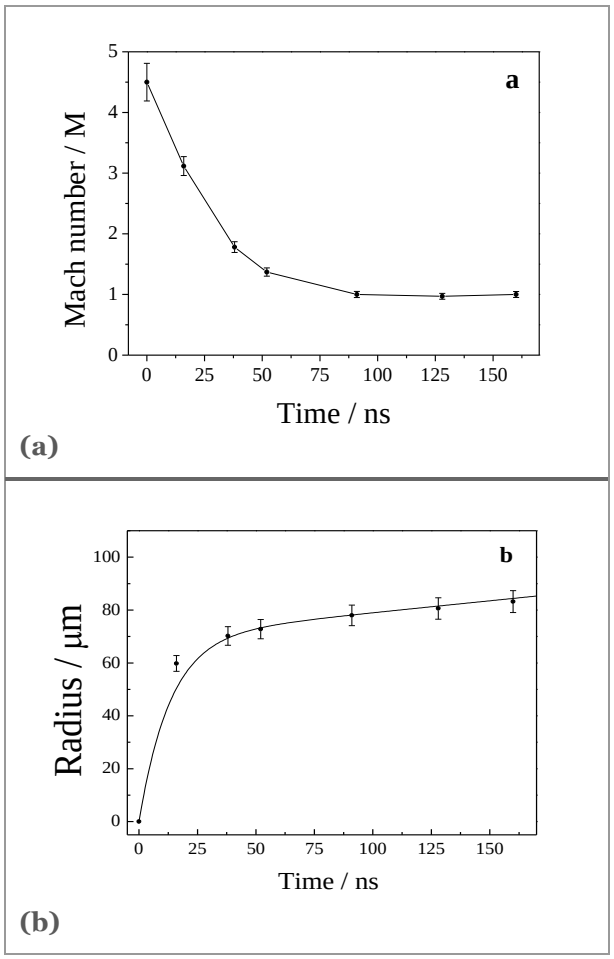

Figure 4: Mach number of spherical shockwaves (a) and the micro-bubbles radii (b) as a function of time. The laser power was 65 mJ.

where $w_0 = 35$ μm is the radial size of the beam at its narrowest point, the Rayleigh length is the distance along the propagation direction of the beam from the waist to the place where the area of the cross section is doubled and $n = 1.33$ is the index of refraction of water [6].
Thus, the concentration of the "breakdowned" inclusion particles might be determined from the quantity of micro-balls in the focal volume:

$$N\,[\mathrm{cm}^{-3}] = B/(2\pi w_0^2 z_R),$$

where B is the number of plasma balls in a laser plasma column. The thus evaluated concentration of the "breakdowned" inclusions in pure and tap water is $N_{pw} \approx 2\text{x}10^4$ and $N_{tw} \approx 3.2\text{x}10^5$ cm^{-3}, correspondently.
The concentration of all particles, not only those breakdowned, might be evaluated by measurements of the 90 degree scattering of the narrow (~1 mm) diagnostic light (λ = 5145 nm). The images of the scattered light from pure (DDW) water and from tap water are shown in Figure 5. They indicate a considerable difference in the concentration of inclusion particles in these liquids.

Figure 5a allows for counting the number of scattering particles in the volume illuminated by the diagnostic beam. The volume was estimated as a cylinder of diameter $d_{1/2} = 0.8$ mm and length of 10 mm, where $d_{1/2}$ is the diameter of the diagnostic laser beam at half of its intensity. The concentration of inclusion particles in pure water was determined as $N_{pw}{}^s = 2.4\cdot10^4$ cm^{-3}. Thus, in pure water the fraction of particles undergoing breakdown is $N_{pw} / N_{pw}{}^s = 0.83$.

The concentration of inclusion particles in tap water cannot be determined directly from Figure 5b, since this value is too large. Therefore, this concentration was estimated using a series of dilutions of tap water in pure water. The obtained value was $N_{tw}{}^s = 1.2\cdot10^6$ cm^{-3}. Thus, in tap water the fraction of particles undergoing breakdown is $N_{tw} / N_{tw}{}^s = 0.27$. The fraction of exploding particles in the focal volume in tap water is remarkably smaller than in pure water. This result might be explained by the differences in the size distribution of particles in these liquids and by the fact that optical breakdown is governed by the biggest inclusion particles.

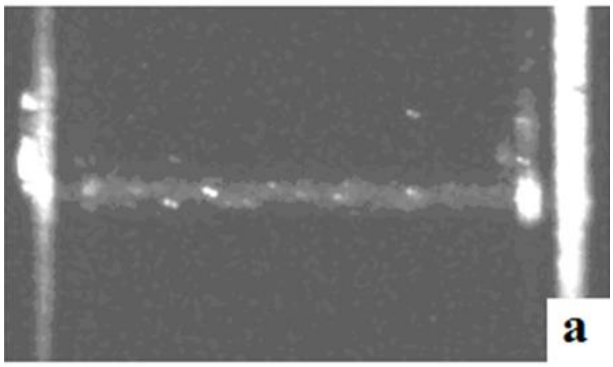

Figure 5a: Image of the light of the diagnostic beam scattered at 90 degrees: DDW. The cuvette size is 10 mm.

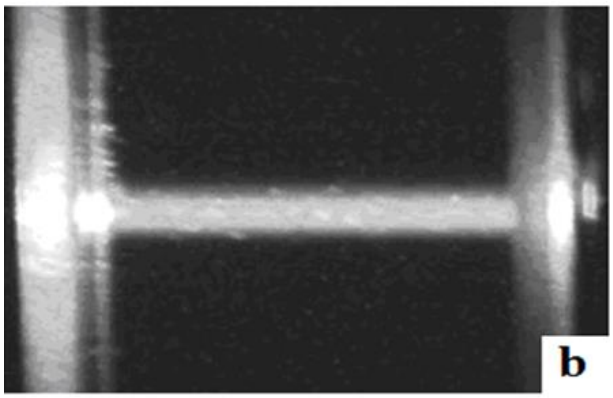

Figure 5b: Image of the light of the diagnostic beam scattered at 90 degrees: tap water. The cuvette size is 10 mm.

3.4 Length of the plasma column in pure and tap water

The length of the plasma column generated in a focused laser bean is affected by the focusing

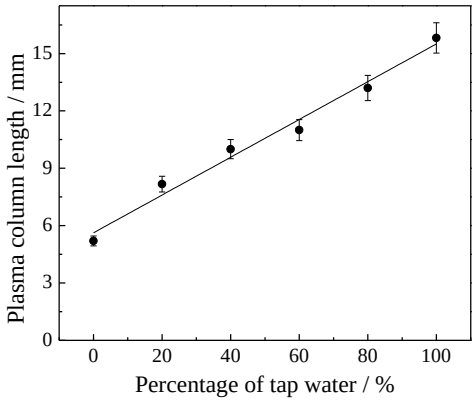

Figure 6: Experimental dependence of the plasma column length as a function of the relative concentration of tap water in mixtures of tap/pure waters.

conditions (Rayleigh length) and by the ratio of the peak power of the laser pulse to the breakdown threshold value. The latter is influenced by the concentration of inclusions, therefore, it is expected that the plasma column length is different in pure and tap waters. A special series of experiments was performed in order to determine the length of a laser plasma column for different mixtures of tap and pure water. The results are shown in Figure 6, where the length of a laser plasma column is presented as a function of the concentration of tap water in tap/pure water mixtures. The energy of the laser pulses was unchanged. The experimental observation is that the plasma column length increases linearly with the concentration of tap water. It is interesting to compare these results with theoretical models.

Previous theoretical and experimental investigations indicated that the plasma profile in liquids is ruled by the moving breakdown model [7-10]. This model assumes that the breakdown occurs independently at each location along the irradiation axis, provided that at that location, the irradiance of the electric field reaches the breakdown threshold value. According to the model, for a laser pulse above the threshold, the plasma is initiated close to the focus as soon as the laser pulse reaches the breakdown threshold, before it reaches its maximum power. At later times during this pulse, as the energy of the pulse increases, breakdown threshold requirements are met at distances further away from the focal point. Hence a dependence of the maximum elongation of the plasma column, $z_{max,}$ can be deduced. Assuming Gaussian distribution of the laser pulse energy the following expression was derived:

$$z_{max} = z_R(\beta\text{-}1)^{1/2} \quad (1)$$

where z_{max} is the length of the plasma column and β is the ratio of the peak power of the laser pulse to the breakdown threshold value.

In order to test this model we first need to obtain the breakdown thresholds in pure and tap waters. As it was already indicated the thresholds depend first of all on the quantity of inclusion particles in the focal volume of the focusing singlet, which is much higher in tap water. Our measurements indicate that pure water exhibits breakdown threshold higher by a factor of ≈3: ε_{th}(DDW) = 15.8 mJ and ε_{th}(TW) = 5.0 mJ. Note that in previous reports it was found that the threshold ration is at least 5 for ns laser pulses [11, 12]. This discrepancy can be attributed to the fact that tap water is not a well-defined medium, however, the difference are not very significant.

Using the experimental threshold values, we could check the validity of Eq.1 for pure and tap waters. The results are shown in Figure 7. The results indicate that the lengths of the laser plasma columns in pure water approximately obey the model of Eq.1. On the other hand, the breakdown in tap water behaves differently and the experimental data are approximately described by the relation:

$$z_{max} \approx 0.7 z_R(\beta\text{-}1)^{1/2} \quad (2)$$

This implies that the effective Rayleigh length in tap water is equal to $0.7z_R$. This result means that the larger concentration of inclusion particles in tap water formally leads to effective diminishing of the Rayleigh length.

3.5 Warmed channels in pure and tap water

Interferometric imaging shows that the optical breakdown in water is realized within a warming region in the focal volume of the focusing singlet. The interference visualizations and measurements allow to determine the size, temperature rising and time evolution of the warmed channels in tap and pure water. These channels are clearly visible in the interferograms presented in Figures 2 and 3. The channels have characteristic diameters of the order of $d_c > 2w_o$. The temperature of the heated water in a channel might be evaluated from the relation:

$$\Delta T = (\Delta n)/(\partial n/\partial T)_\rho \quad (3)$$

where $(\partial n/\partial T)_\rho$ = -0.8·10^{-4} K^{-1};

Δn is the change of the refraction index of water, which can be calculated from the interferograms:

$$\Delta n = \Delta k\lambda / d_c \quad (4)$$

where λ = 532 nm is the wavelength of diagnostic light and Δk is the fringe shift. For Δk_{max} = 0.5 the temperature change is $\Delta T \approx 10$ K.

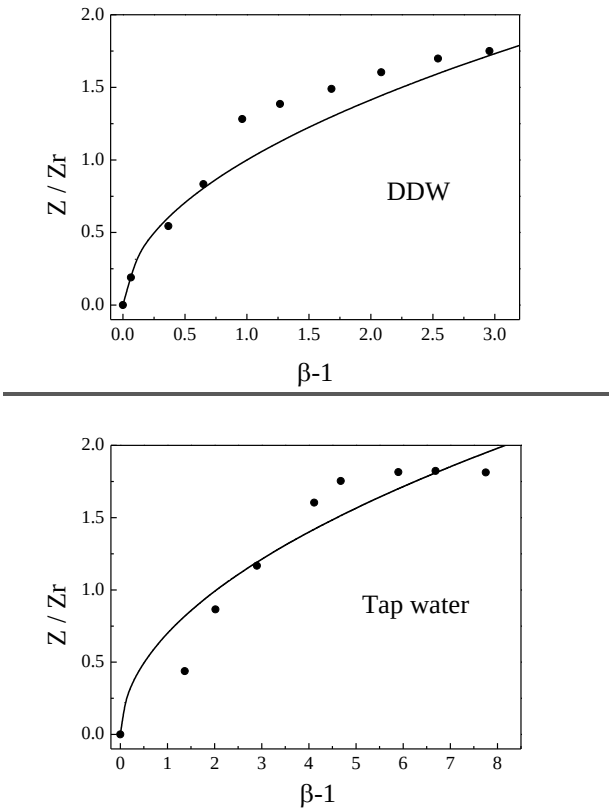

Figure 7: Normalized length of the laser plasma column as a function of (β-1) for pure and tap water. The solid lines describe the model: $(\beta-1)^{1/2}$ for DDW and $0.7(\beta-1)^{1/2}$ for tap water.

On the other hand, the temperature of water might be approximated from the following simple considerations. The laser pulse energy ε_a, is absorbed in a cylindrical volume of diameter d_c in a liquid of extinction coefficient α = 0.15 cm^{-1}. The absorbed energy is calculated according to the Beer-Lambert law. From the law of conservation of the energy the warming (ΔT) might be evaluated using the equation:

$$\Delta T = \frac{\varepsilon_a \alpha}{\rho c S} \qquad (5)$$

where ρ = 1 [g·cm^{-3}] is the density of water, c = 4.18 [J.g^{-1}.K^{-1}] is the heat capacity of water and $S = \pi(d_c/2)^2$. The average temperature change of the water in the channel is evaluated from Eq. 3. For ε_a = 10 mJ we find $\Delta T \sim 9$ K. This value is close to that obtained from the interferometric measurements. No significant differences between pure and tap waters were observed.

The interferograms allow for time dependent temperature estimation. It has been found that the warmed channels in both water samples last for times $\tau_d \geq 1$ μsec. Thus, one can conclude that they are deactivated by the relatively long process of thermal conductivity.

CONCLUSIONS

The mechanism of the optical breakdown by ns pulses of λ = 1064 nm in tap and pure water was investigated. Clearly, the breakdown is initiated by inclusion particles, of which concentration is different in the various water samples. The structure and dynamics of the laser plasma columns in tap and pure water were numerically determined from interference measurements.

The fraction inclusion particles undergoing breakdown in the studied samples was estimated from the concentration of micro plasmas and the total concentration of particles. This fraction is lower in tap water than in pure water. This result was attributed to the differences in the size distribution of particles in these liquids and to the fact that optical breakdown is governed by the biggest inclusion particles.

The plasma column length was measured is a series of mixtures of tap and pure water. The results were compared to theoretical models. While pure water is reasonably described by the moving breakdown model, a modified expression was needed for the tap water case.

Warmed channels in both liquids were observed for a rather long duration. The temperature change was numerically evaluated.

REFERENCES

[1] C.E. Bell, J.A. Landt, *Appl. Phys. Letts* **10** (2) 46 (1967)

[2] G.A. Askar'yan, A.M. Prokhorov, G.F. Chanturiya and G.P. Shipulo, *Sov. Phys. JETP* **17**, 6 (1963)

[3] G. Toker, V. Bulatov, T. Kovalchuk, I. Schechter, *Chem. Phys. Letts* **471**, 244 (2009)

[4] T. Kovalchuk, G. Toker, V. Bulatov, I. Schechter, *Chem. Phys. Lett.* **500** 242 (2010).

[5] Y.P. Raizer, "Laser-Induced Discharge Phenomena", Consultants Bureau, N.Y., London, (1977)

[6] J.N. Damask, "Polarization Optics in Telecommunications", pp. 221–223, Springer (2004). ISBN 0-387-22493-9.

[7] A. Vogel, K. Nahen, D. Theisen, and J. Noack, *IEEE Jour. of Selec. Topics in QE*, **2**(4), 847 (1996).

[8] E.N. Glezer, C.B. Scgaffer, N. Nishimura, E. Mazur, *Optics Letters*, **22**(23), 1817 (1999).

[9] F. Docchio, P. Regondi, M.R.C. Capon, J. Mellerio, *Appl. Opt.*, **27**(17), 3661 (1988).

[10] F. Docchio, P. Regondi, M.R.C. Capon, J. Mellerio, *Appl. Opt*., **27**(17), 3669 (1988).

[11] F. Docchio, A. Avigo and R. Palumbo, *Europhis. Letts*, **15**(1), 69 (1991).

[12] F. Docchio, A. Sacchic and J. Marshal, *Lasers in Ophthalmology*, **1**, 83 (1986).